Fuel 371 (2024) 132049

Contents lists available at ScienceDirect

Fuel

journal homepage: www.elsevier.com/locate/fuel

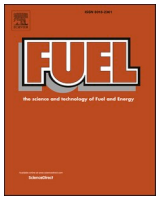

Full Length Article

The effect of theoretical SAF composition on calculated engine and aircraft efficiency

Randall C. Boehm [a,*], Conor Faulhaber [b], Lily Behnke [c], Joshua Heyne [a,b,d]

[a] Washington State University, Bioproducts Sciences and Engineering Laboratory, School of Engineering and Applied Science, Richland, WA 99354, United States
[b] Washington State University, Bioproducts Sciences and Engineering Laboratory, Department of Biological Systems Engineering, Richland, WA 99354, United States
[c] University of Dayton, Department of Mechanical & Aerospace Engineering, 300 College Park, Dayton, OH 45469, United States
[d] Pacific Northwest National Laboratory, Energy Processes and Materials Division, Energy and Environment Directorate, Richland, WA 99352, United States

ARTICLE INFO

Keywords:
Sustainable Aviation Fuel
Energy Efficiency
Composition Optimization

ABSTRACT

Whether the feedstock for sustainable aviation fuel (SAF) originates from agriculture or from waste streams, life cycle CO_2 emissions per unit enthalpy are lower for SAF than they are for petroleum distillates primarily because of differences on the front end such as fostered growth of crops or decreased demand for resources or acreage to manage wastes. This work, however, is concerned with what happens on the consumption side. Sustainable aviation fuel is required by ASTM D4054 / D7566 to meet a higher thermal stability standard than petroleum distillate fuels and this characteristic can be leveraged to improve energy efficiency in new engine or aircraft designs where a commitment has been made to burning fuel that meets a specification beyond that of conventional JetA. Beyond thermal stability, non-drop-in SAF (Jet-X) developers have the opportunity to further increase the value of their product by infusing higher-than-conventional-JetA energy density (enthalpy per unit volume, ED) into their SAF. Finally, fuel specific energy (enthalpy per unit mass, LHV) has a direct impact on aircraft efficiency which we have determined to be 0.43% per MJ/kg increase in LHV depending on the mission and aircraft model, and this is applicable to both drop-in and non-drop-in applications. While higher energy density fuels may be leveraged in a new aircraft design to decrease drag and weight, aircraft development potential with reduced tank volumes is typically constrained by other factors such as wing packaging, passenger volume requirements and overall center of gravity and flight control law restrictions.

1. Introduction

As the global population and its demand for energy and transportation continue to rise, the environmental impact from combustion systems that satisfy that demand is of growing concern [1,2]. In response to this concern, several U.S. federal agencies are working collaboratively to facilitate execution of the Sustainable Aviation Fuel (SAF) Grand Challenge [3] which is a comprehensive plan to achieve net zero CO_2 emissions from the aviation sector by 2050. While the aviation sector is pursuing a combination of approaches, including aircraft technology, operational improvements, and carbon offsetting to meet the net zero emission target, SAF is an integral piece of that plan. Three key objectives pertaining to SAF are identified in the plan:

1. expanding its supply and end use
2. reducing its cost
3. enhancing its sustainability

The topics of this article touch upon each of these objectives. To expand usage, it will likely become necessary to qualify new or existing SAF beyond the current maximum blend percentages in ASTM D7566 as the industry gains familiarity with the fuels and trust in the evaluation process. Optimizing SAF compositions provides targets for fuel producers to tune their processes towards products that are well-positioned to successfully navigate the certification process at blend ratios potentially up to 100 %. Alternatively, or in parallel, certain aircraft could be certified or re-certified on fuel (called Jet-X in the remainder of this document) containing any amount of SAF provided a quality control specification for that fuel has been approved by all of the aircraft's stakeholders. Such aircraft would not necessarily be certified to operate

* Corresponding author at: Washington State University, Bioproducts Sciences and Engineering Laboratory, School of Engineering and Applied Science, Richland, WA 99354, United States.
E-mail address: randall.boehm@wsu.edu (R.C. Boehm).

https://doi.org/10.1016/j.fuel.2024.132049
Received 4 December 2023; Received in revised form 25 March 2024; Accepted 28 May 2024
Available online 1 June 2024

on conventional fuel and hence may be restricted to operations between airports having access to Jet-X. Supersonic aircraft provide a real-world and current example of aircraft that are expected to be deployed at targeted airports around the world. Therefore, model supersonic aircraft and missions are used here to characterize the potential benefits of Jet-X, adding value to the synthetic fuel thereby effectively reducing its operating cost. Beyond the overall effort of increasing the percentage of renewable carbon in onboard jet fuel, this work specifically enhances fuel sustainability by optimizing on enthalpy savings and highlighting emissions impacts of the proposed compositions via threshold sooting index (TSI) predictions.

Previously, Kosir et al [4,5]. optimized energy density and specific energy and characterized the fuel savings as 2.8 %m (1.2 % by enthalpy) resulting solely from a 1.6 % decrease in fuel weight at take-off, for a Boeing 737–800 flying from New York to San Francisco. Kroyan et al [6]. has observed that variation in enthalpy consumption at cruise conditions across 55 flights (−2.03 % to + 2.94 % relative to a baseline JetA-1 fuel) correlates strongly with variation in three fuel properties; LHV, density, and viscosity. Boehm et al[7]. showed that changes in fuel properties, most notably viscosity and hydrogen to carbon ratio (H/C), impact specific fuel consumption (SFC) via changes in waste heat recovery and work extracted by the turbine of a jet engine. Without any change to engine or aircraft design or mission profile, a set of 2,500 random fuels showed approximately a 0.15 % range in energy consumption relative to the reference fuel designated as A-2 [8] which was defined by a committee of engineers from competing engine manufacturers and procured by the U.S. Air Force prior to the beginning of the National Jet Fuel Combustion Program [9]. Unfortunately, the property variation (low end of H/C) that affords more efficient work extraction from the turbine is opposite from the variation (high end of H/C) that affords lower fuel weight (higher LHV). Clearly, the impact of fuel weight is more significant, but the debit of higher H/C as it relates to work extraction from the turbine should be considered.

The lower end of the viscosity variation was shown previously [7] to be beneficial with respect to waste heat recovery, which improves engine-level energy efficiency, and fuel atomization [10]. However, the increased waste heat recovery due solely to the viscosity effect on heat transfer, through Reynolds number and Prandtl number dependencies, has a much smaller (less than 10 %) impact on SFC than can be expected from straight-forward changes to the thermal management design of the engine. Boehm et al. showed that an increase in fuel temperature from 127 °C to 160 °C would result in energy savings of 0.2 % even if no other benefits are credited, and the potential reduction of air pressure losses levied on the engine by the thermal management system could result in an additional 0.3 % savings. These larger benefits require a design change to increase the fuel temperature, and since a design change is required to get this benefit, temperatures beyond 160 °C should be explored.

The maximum fuel temperature attained in jet engines and at the inlet to the jet engine is restricted by design to avoid three technical risks: exceedance of material temperature limits (particularly elastomeric O-rings), exceedance of the fuel bubble point (particularly at low fuel flow where fuel pressures are lowest and fuel temperatures, historically, are highest), and thermal oxidation of the fuel resulting in deposits (called coking) that can adversely impact valve operability, spray quality, combustor pattern factor and the maximum fuel flow rate capability of the engine [11]. For reference, the bubble point is the temperature (at a given pressure) where the first bubble of vapor is formed when heating a liquid consisting of two or more components. The production of novel SAF products offers an opportunity to improve the overall thermal stability of jet fuel and reduce coke build-up which, in turn, could reduce airline maintenance costs. The exact savings benefit from this aspect of SAF is not yet quantified and thus warrants further investigation from stakeholders.

The maximum fuel temperature, 160 °C, considered by Boehm et al. is approximately the same number as would be derived from any one of the three technical risks mentioned above. The coking risk has been already mitigated for Jet-X by increasing the quality-control specification temperature, found in ASTM D3241/D7566, from 260 °C to 325 °C or higher, and through the growing understanding of the impact of trace contaminants on thermal stability. The material limitation can be pushed to higher temperature by choosing elastomeric materials that are more resilient to temperature than historically chosen materials or designing a fuel system in which any valve with an O-ring is placed upstream of major heat sources. The bubble point is less of a concern when the fuel pressure is well above the critical pressure of fuel (for reference: n-dodecane has a critical pressure of 18.0 ± 1.4 atm [12]), but at high-altitude and low-flow operating conditions (such as the chop from sub-sonic cruise to flight idle and the top of descent) the fuel pressure is below its critical pressure. Thermal management systems that preferentially leverage fuel cooling while the aircraft is operating under conditions of high fuel pressure would avoid the technical risks born from incipient boiling.

The combustor operating pressure and the fuel flow rate at supersonic cruise conditions are relatively high and therefore the fuel pressure inside the fuel system, from boost pump to combustor, is relatively high and is conservatively estimated as 25 atm for the purpose of this work. The limiting Jet-X temperature at this condition is therefore taken to be the temperature at which its vapor pressure reaches 25 atm. In contrast, the limiting Jet-X temperature for the throttle chop transient from cruise to flight idle (Mach < 0.1), where the fuel flow rate and combustor operating pressure are at their lowest, is the bubble point of the fuel at 1.75 atm (estimated). Depending on thermal management system architecture, either of these two mission points, supersonic cruise or the chop from sub-sonic cruise to flight idle, could be limiting with respect to maximum allowable fuel temperature and therefore both are considered in this work.

This investigation utilizes fuel composition optimizations to assess SAF candidates that will add value in terms of engine efficiency, aircraft efficiency and reduced coking. Some of these fuels are envisioned as drop-in aviation fuels at any blend fraction with any other aviation fuel, while others may have some properties (e.g., minimum aromatics content or maximum energy density) that are outside of the guidelines described in ASTM D4054. Specific objective functions (a.k.a. cost functions) included in the dual-objective optimizations are LHV, energy density, vapor pressure at 200 °C, engine enthalpy savings relative to the reference fuel [8] designated A-2, and aircraft enthalpy savings relative to the reference fuel. The methodology used to translate fuel properties into engine enthalpy at specific operating points (a.k.a. mission points) is described elsewhere [7] while the weighting of specific mission points used to represent a full mission (a.k.a. mission mix) is described in the methodology section of this manuscript. Also described here is the methodology used to translate fuel properties into aircraft relative enthalpy savings (ARES).

In another section, fuel composition characteristics, such as hydrocarbon class (e.g. cycloalkane, alkylbenzene, etc.), molecular weight, branching, and ring size of species favored by the optimization are summarized. Moreover, the most favored species within each category is reported. The motivations here are 1) to inform SAF producers of specific molecules or molecular characteristics that should be targeted during the conceptual phase of their technology development plan and 2) to identify specific molecules or molecular characteristics that should be evaluated experimentally, including implications regarding thermal stability, elastomer material compatibility and other difficult-to-predict fuel properties.

Overall, the results of this work will extend the current capabilities of SAF from a performance standpoint while also leading to a greater understanding of effects that currently lead to maintenance and emissions issues in modern aircraft.

2. Methodology

2.1. Optimization logic

A flowchart outlining the optimization logic is shown in Fig. 1. The process begins by assigning a random number between 0 and 1 to each molecule in the database which is described in section 2.2, and then clipping to zero all values that were less than 0.75. This is done to limit the number of molecules that comprise each candidate fuel. Next, the assigned number is divided by 33.3, 4, or 2 if the associated molecule has a threshold sooting index (TSI) above 75, 30, or 15, respectively. This is done to increase the probability that a trial fuel will have lower sooting propensity than conventional jet fuel in spite of the database containing a disproportionate number of alkylated naphthalenes (7 %) and benzenes (29 %). Next, this set of numbers is normalized so they sum to one, and these represent the mole fraction of the associated molecule in the trial fuel. Together with a database of molecular properties, these trial fuel compositions are input into a subroutine to predict all of the fuel properties listed in Table 1 [13–16]. These predicted properties are then compared against limit constraints taken from ASTM D1655 or as described here. The upper limit vapor pressure at 160 °C is set to 1 atm. to mitigate the risk of a phase change within the fuel system. We presume, at this point, that any trial fuel that passes this constraint will also have a flash point that is higher than 38 °C and this presumption is checked for candidate fuels that are suggested by the optimization routine. The T_{10} ruler is a surrogate requirement for the T_{10} upper limit which is 205 °C, where the ruler is the sum of mole fractions over all fuel components that have a normal boiling point less than 205 °C. The actual T_{10} of candidate fuels is calculated after the optimization, assuming the distillation has just one theoretical plate, similar to ASTM D86 which is one of the distillation methods called out in ASTM D1655. The TSI upper limit is set to 20, which corresponds to a smoke point of 25 mm for a fuel with a molecular weight of 170 g/mol. This constraint is a surrogate for the smoke point requirement that is expressed in ASTM D1655. Five of these six properties are limited by the fuel specification at one end only, while density has both an upper and lower bound.

If a trial fuel composition fails to express properties that meet all seven constraints, then it is discarded without any further drain on computational resources. At that point, the logic returns to the trial fuel generator. The trial fuel generator consists of two parts. In the 'random' portion of the routine an all-new trial fuel is created as described above, and this process continues until a user-defined target number of kernels have been created. Note the usage of 'trial fuel' and 'kernel'. A trial fuel is defined here as any hydrocarbon mixture, generated at random. A kernel is a hydrocarbon mixture that satisfies all seven constraints. The last set of kernels derived by the optimizer are 'candidate fuels'. In the 'derivative' portion of the trial fuel generator, a random modification is made to a randomly selected kernel. The user supplies input to the routine to inform the maximum number of changes (N) to consider and the maximum step size (S). A subroutine then picks an integer (n) between 1 and N and associates a step size (s), between −S and S, with each one. Any resulting mole fraction that falls below a user-supplied threshold value (e.g., 0.00015) is set to zero. Upon completing all of the modifications, the mole fraction vector is renormalized to one. In this investigation, the number of kernels was set to 250 for most optimizations, N was set to 5 and S was set to 0.01.

Table 1
Summary of Predicted Properties of Trial Fuels (Pre-Filter).

Vapor Pressure @ 160 °C	Density @ 15 °C
Kinematic Viscosity @ −20 °C	LHV
T_{10} ruler[†]	TSI

[†] T_{10} ruler is defined as a mole faction sum, over molecules with normal boiling point less than 205 °C

Kernels (a.k.a. trial fuels that pass all seven constraints) are sent to the most computationally intensive subroutine where additional fuel properties are predicted, including most notably the fuel impact on engine-level enthalpy consumption. These additional properties are summarized in Table 2. The temperature dependence of heat capacity, thermal conductivity, molar volume, and the log of dynamic viscosity was derived by fitting a line through five points (15, 50, 85, 120 and 155 °C), where the property value at each of these five temperatures was found by taking the scalar product of the mole fraction vector and the corresponding property vector from the database. These properties, along with molecular weight are required to execute heat transfer calculations which are referenced in sub-section 2.3. The hydrogen to carbon ratio, and molecular weight to a lesser degree, are required to determine extractable work from an adiabatic expansion, which is also referenced in section 2.3. The remaining four properties listed in Table 2, as well as LHV, are objective functions. Any pair of objective

Table 2
Summary of Additional Properties Necessary to Evaluate Objective Functions.

Temperature Dependent Heat Capacity	Temperature Dependent Molar Volume
Temperature Dependent Dynamic Viscosity	Temperature Dependent Thermal Conductivity
Hydrogen to Carbon Ratio	Molar Mass
(optionally) Energy Density @15 °C	(optionally) Vapor Pressure @200 °C
Engine Relative Enthalpy Consumption	Aircraft Relative Enthalpy Consumption

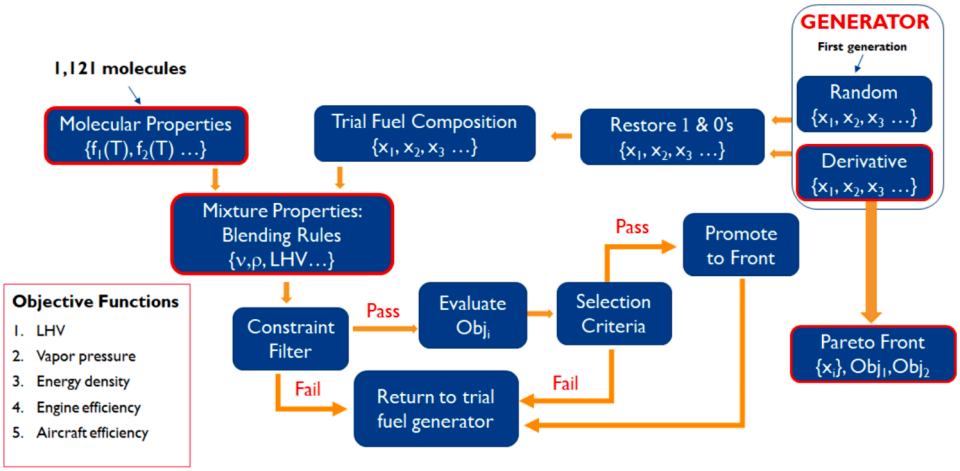

Fig. 1. Fuel Optimization Logic.

functions may be optimized simultaneously. The engine relative enthalpy savings (ERES) is the main topic of section 2.3. Vapor pressure is estimated by combining Dalton's Law and Raoult's Law with the Clausius-Clapeyron equation, where Trouton's Rule was used to estimate the heat of vaporization of each molecule in the database. The aircraft relative enthalpy savings (*ARES*) was estimated by equation 1, where *ERES* is the engine relative enthalpy savings, WFE is the fuel flow, 43.058 MJ/kg is the LHV of the reference fuel, and 0.0043 is a scalar derived from data supplied by Boom Technology, Inc. (Boom) that summarizes the impact of fuel weight at takeoff for typical *trans*-ocean missions (represented by Vancouver-Tokyo and New York-London). The proprietary models used by Boom to generate this data are briefly described in section 2.7, while an independent derivation relating the fuel weight during cruise to the enthalpy necessary to complete the cruise leg of the mission is provided in the supplemental material: entitled, "fuel weight impact on cruise enthalpy demand".

$$ARES = ERES + 0.0043*(LHV - 43.058) \tag{1a}$$

$$RelativeEnthalpySavings \equiv 1 - \left(\frac{WFE}{WFE_{ref}}\right)*\left(\frac{LHV}{LHV_{ref}}\right) \tag{1b}$$

The selection subroutine compares each new kernel, sequentially by index, to kernels that are stored in the dynamic pareto front. If a kernel's corresponding objective functions are both determined to be more favorable than those of at least one other kernel, the inferior kernel's mole fraction vector is overwritten by that of the new kernel. At this point, the logic returns to the trial fuel generator thereby completing a loop which continues until the user-specified iteration limit is reached. Upon completion of the iteration loop, the dynamic pareto front is written to file, enabling the user to monitor how much the objective functions, constrained properties, unconstrained properties and composition change from generation to generation.

2.2. Database

A wide array of molecules was selected to appeal to the sensitivities of fuel property models and the impact of fuel properties on enthalpy savings. The NIST standard reference database [12] was leveraged as the source database for the properties required by the optimization routines. This database was filtered to contain only alkanes, mono-, bi- or tricycloalkanes excluding any with 3- or 4-membered rings, alkylbenzenes, indanes or tetralins, and alkyl naphthalenes having a normal boiling point in the range, 79–300 °C. The upper limit of this range matches the aviation fuel specification upper limit on distillation end point while the lower limit of this range was chosen for expedience; in anticipation of our internally imposed bubble point limit or the ASTM D1655 flash point limit being a property that would constrain the optimization. Each of the retained molecules had reported data for each of the properties listed in Tables 1 and 2 over the temperature range 15–155 °C that was selected to represent the temperature dependence of the properties including, heat capacity, thermal conductivity, molar volume, viscosity and vapor pressure. Since the analysis for each trial fuel required a property value at any arbitrary temperature value in this range and a few discrete points (−40, −20 & 160) outside of this range, the curve fits as described in section 2.1 were regenerated for each trial fuel while the noted blending rules were used to create the five basis points for each trial fuel property. Finally, thirty-six molecules were filtered out of the database because one or more of the reported properties of the molecule was determined by visual inspection of histograms to be an outlier. Specifically, the properties considered for this operation included LHV and the first derivative with respect to temperature of density, heat capacity, thermal conductivity, and log viscosity. After filtering, 1121 molecules remained in the database.

2.3. Engine, relative enthalpy savings

The fuel effect on jet engine efficiency is not usually considered by engine manufactures as their performance models employ reference fuel properties. From this perspective, a jet engine is just an air breathing machine whose thrust is manufactured by expelling air at a higher velocity than it ingests air. Fuel combustion is used to change the density of the fluid passing through the turbine and exhaust nozzle by increasing its temperature. Within this simplified perspective the temperature rise across the combustor is determined by the thrust demand arising from the flight mission point and is physically the result of continuously burning some mass flow rate of fuel (WFE) having a specific energy (LHV). If the LHV of the actual fuel is higher than the LHV of the reference fuel, then the actual flow rate of fuel will be lower than the reference (or demanded) flow rate necessary to achieve the thrust required to achieve the intended flight conditions. Alas, this simplified perspective neglects the fact that the composition of the fluid exiting the engine is not exactly the same as the air it ingests. In actuality, the temperature rise across the combustor also depends somewhat on the inlet fuel temperature, its flow rate and the thermal properties of the vitiated air. Additionally, the work extracted by the turbine also has a second-order dependence on vitiated air thermal properties. Moreover, the combustor inlet fuel temperature depends on its flow rate and its (liquid) thermal and fluidity properties (heat capacity, conductivity, viscosity). While each of these fuel effects on jet engine performance are touched upon again in the next two paragraphs, readers who desire full detail are referred to the python source code (called class_surrogate.txt) which is provided in the supplemental material.

As a means to estimate fuel effects on jet engine fuel efficiency, Boehm et al. [7] created an engine performance model (EPM) that captures, on the air side, two stages of adiabatic compression with cooling flow extracted after each stage, combustion, and adiabatic expansion. The fuel enthalpy is treated as an input to the EPM within the combustion module. A separate model, called the fuel system thermal model (FSTM), was developed to estimate heat absorption by the fuel while passing between the fuel tank and the combustor. The base FSTM consists of five heating elements: the aircraft fuel system (tank to engine inlet), the main engine fuel pump, a recirculation loop, the fuel-cooled oil cooler, and the rest of the engine fuel system. An optional sixth heating element, a fuel-cooled air cooler, was developed to assist in the exploration of conceptual designs for a thermal management system. The user-defined inputs to these models include pressure ratios, air flow splits, reference fuel flow rate, bypass loop fuel flow split, and engine-inlet air flow rate. The developer inputs include the hydraulic diameter, coil diameter and length of each heating element. Boehm et al. published the complete set of developer inputs and user inputs corresponding to a low-power mode of operation and a high-power mode of operation. Their low-power model was intended to represent the transition from cruise to flight idle, which is usually the operating condition where the fuel temperature reaches its highest value. Their high-power model was intended to represent sea-level take-off of a fully loaded aircraft.

The main fuel property effect on heat transfer is viscosity, where lower viscosity promotes higher turbulence and heat flux, and the primary reason for this is that viscosity is significantly more sensitive to variation in both composition and temperature than other relevant properties such as liquid-phase heat capacity, thermal conductivity, and energy density (which effects volumetric flow rate). [17] The main fuel property effect on work done by adiabatic expansion is the hydrogen to carbon ratio (H/C). This can be seen through examination of equations (2) through (5), where the subscripts *4* and *8* refer to the turbine entrance or exit stage, respectively, and the subscripts *reac* or *prod* represent the reactants or products of combustion, respectively. In these equations, n represents moles, H represents enthalpy, T represents temperature, P represents pressure, n_H represents the average number of hydrogen atoms per mole of fuel, and C_p *or* C_v represents molar heat

capacity at constant pressure or volume, respectively. The hydrogen to carbon ratio of the fuel impacts the composition of the product gas (the relative amount of H_2O and CO_2), thereby affecting the heat capacity of the product gas.

$$\Delta H_{expansion} = \int_{T_4}^{T_8} \dot{n_{prod}} * Cp_{prod} dT \tag{2}$$

$$\frac{T_8}{T_4} = \left(\frac{P_8}{P_4}\right)^{\left[\frac{(1-\gamma_{prod})}{\gamma_{prod}}\right]} \tag{3}$$

$$\gamma \equiv C_p / C_v \tag{4}$$

$$n_{prod} = n_{reac} + \left(\frac{n_H}{4} - 1\right) | equivalenceratio = 0.5 \tag{5}$$

The turbine inlet temperature, the ratio between the turbine exit and entrance temperatures, and the particulate matter resulting from fuel combustion are all impacted by H/C in a manner that has competing influence on the enthalpy extraction available to do mechanical work. Boehm et al. [7] found that a large (17 %) decrease in H/C results in a small (0.06 %) increase in the total work available via adiabatic expansion, but after subtracting the work required to compress the air going into the combustor the percentage increase in energy available to create thrust increased by 0.44 %. That is a significant number, but unfortunately in the opposite direction from what we would like vis-a-vis fuel weight at takeoff and particulate emissions. In other words, fuels that are advantageous with respect to aircraft fuel efficiency and environmental impact are detrimental with respect to jet engine fuel efficiency. This debit is not large, but it should be and is considered in the comprehensive assessments of the benefits of optimized, hypothetical SAF that are reported in this article.

2.4. Mission mix

The magnitude of ERES varies with engine operating conditions (fuel flow and fuel to air ratio) [7], which, in turn, vary with aircraft operating conditions such as altitude, airspeed, and thrust. The one aircraft condition that strongly influences engine conditions including fuel flow rate among others is its thrust demand. For the purpose of this investigation Boom provided two mission profiles (time increment, fuel flow rate, thrust, etc.) represented by over 3000 discrete points. The relative fuel flow, expressed as a ratio (R_i), at each of these mission points was approximated by equation (6), where thrust is represented by F and the subscripts refer to the discrete point index, the minimum or the maximum engine operating conditions.

$$R_i = R_{min} + (R_{max} - R_{min}) * (F_i - F_{min}) / (F_{max} - F_{min}) \tag{6}$$

The ratio of fuel flow at minimum or maximum flow conditions is taken from the model described in section 2.3. This approximation works out to a net weighting of 69 % at minimum power and 31 % at maximum power for the *trans*-Atlantic mission. For sub-sonic short-haul flights employing a Boeing 737, we estimate net weighting of 50 % at minimum power, and this is the number used within the inner loop of the optimization to estimate ERES for each kernel fuel. By choosing 50 % instead of 69 % weighting of the minimum operating condition, we are biasing the pareto front somewhat toward that of conventional jet fuel, at least with respect to H/C. This is because R_{max} is very strongly determined by H/C while R_{min} is also influenced significantly by variation in waste heat recovery which is driven primarily by viscosity variation as a function of fuel composition. In the final assessment, discussed later in this report and centered around Jet-X benefits for supersonic aircraft, the 69 % weighting of R_{min} is used. As the composition characteristics of pareto front fuels are described in section 3.3 it will become clear that optimal fuels are pushed toward maximum H/C even with the artificial bias we impose toward lower H/C.

2.5. Convergence and database selection

Three optimizations started with 1121 molecules in the database. One of these iteratively maximized LHV and ERES, another maximized ARES and energy density (ED), and the other maximized ARES while minimizing the vapor pressure (P_{vap}) at 200 °C. For each of these optimizations, the number of iterations required to achieve convergence was reduced by trimming molecules from the database based on their absence from any kernel fuels found within the dynamic pareto front after 5–10 generations where each new generation is the result of 5000–10000 trial fuels. In the LHV/ERES optimization, this step was repeated twice, resulting in a database of 189 molecules in the final stages of the optimization. The ARES/ED and ARES/P_{vap} optimizations ended with 210 and 261 molecules, respectively, retained in the final databases. Upon trimming the database, each optimization was restarted from scratch, that is, from randomly guessed mole fractions of molecules in the trimmed database. Convergence was declared when the pareto front of the n^{th} generation of 2,000 trial fuels presented both a minimum and maximum ARES value that was displaced by less than 0.01 % relative to the $(n\text{-}1)^{th}$ generation and the following other numerical characteristics also presented. No point on a converged pareto front was below and to the left of any other point on the front and fewer than 10 % of the trial fuels were identified as kernels and subsequently promoted to the front.

Interim optimization results revealed sensitivities that warranted consideration of other databases. In light of this, five database sub-sets were considered to illuminate notable differences between hydrocarbon types. These databases are listed here.

a. filtered to include only cycloalkanes (1, 2 or 3 rings)
b. filtered to exclude all cycloalkanes
c. filtered to include only mono-cycloalkanes
d. filtered to include only *iso*-alkanes having exactly one branch
e. single-branch *iso*-alkanes plus ethyl benzene, with the initial guess being the kernels from d, modified by seeding with 1–20 % ethylbenzene

2.6. Property and composition analysis of candidate fuels

In addition to the six properties listed in Table 1 and the ten properties listed in Table 2, several additional property estimates were made for the purpose of comparing candidate fuels with conventional fuels. These properties are listed in Table 3. The thermal diffusivity, Prandtl number, Ohnesorge number and smoke point are all calculated from other fuel properties. Surface tension was approximated by equation (7) [18] where $\vec{X}$ represents the mole fraction vector and $\vec{\sigma}$ represents the components' surface tension vector. Missing elements in the property vector were set equal to the mean of similar molecules (same type and carbon number) for which data does exist in the DIPPR [19] database. The freeze point model described by Boehm et al. [20] as well as the seal-swell work of Faulhaber et al. [21] were used here for guidance relating to freeze point risk and elastomeric material compatibility risk, respectively. The distillation features are approximated through

Table 3
Summary of Additional Properties Used to Evaluate Candidate Fuels.

Temperature dependent thermal diffusivity	Temperature dependent Prandtl number
Temperature dependent surface tension	Temperature dependent Ohnesorge number [1]
Temperature dependent vapor pressure	Distillation features (T_{10}, T_{30}, T_{50}, T_{70}, T_{90})
Smoke point	Seal swell [2]
Kinematic viscosity at −40 °C [2]	Freeze point [2]

[1] Excluding the characteristic length (e.g. droplet diameter)
[2] Qualitative prediction here to be followed by measurement

simulation of a still with one theoretical plate, using Dalton's Law and Raoult's Law along with the Clausius-Clapeyron equation and Trouton's Rule to determine vapor pressure as a function of liquid-phase composition and temperature.

$$\sigma_{fuel}^{0.25} = \langle \vec{X} | \overrightarrow{\sigma^{0.25}} \rangle \quad (7)$$

Dimensions of the composition analyses include carbon number, hydrocarbon type or degree of unsaturation ($2*n_C + 2 - n_H$), saturated ring size if present and the extent of branching in alkyl groups. Any specific molecule that is found in any one candidate fuel at a mole fraction above 0.1 or is found on average over all candidates within a pareto front at a mole fraction above 0.05 is highlighted separately because these are molecules that we specifically recommend as target products for fuel producers.

2.7. Aircraft relative enthalpy savings

Proprietary models developed by Boom Technology, Inc., were used to derive linear relationships that relate changes in aircraft weight and drag components to changes in mission fuel consumption, to assess sensitivities. The weight derivative is used to evaluate changes in mission fuel weight (LHV) to aircraft component sizing differences vis-a-vis heat exchangers, fuel tanks, the fuselage, wings and engine based on revised fuel burn requirements. In total, seven cases have been considered. Configuration B/L is the baseline design, which is compatible with conventional fuel or drop in SAF. Configuration A incorporates efficiencies of reduced fuel weight made possible by a steady diet of Jet-X with 2 % (or more) higher LHV than the reference fuel allowing the aircraft to reduce fuel weight while maintaining overall range. Configuration B incorporates resizing of the central fuel tank, fuselage, wings and engine to exploit a steady diet of Jet-X with 8 % (or more) higher ED than the reference fuel without consideration of alternative aircraft volume requirements such as passengers, cargo, and systems. Configuration C combines aircraft resizing of configuration A & B, consistent with Jet-X with 1 % higher LHV and 4 % higher ED. Configuration D evaluates the technical feasibility of using fuel as the coolant for the (cabin) environmental control system (ECS). Configuration E evaluates the technical feasibility of using fuel as the coolant in the ECS precooler. Configuration F evaluates the merit of using fuel (instead of air) as the coolant in the hydraulic system.

3. Results

3.1. Summary of aircraft design Trade studies

The results of trades studies considering different aircraft architectures intended to leverage Jet-X properties are provided in Table 4. It must be noted that results presented in Table 4 are optimistic, and achievable benefits may be limited in practice. Further, while mission benefits are reported in terms of both increased range and improved fuel efficiency, they are mutually exclusive to one or the other, but not both. Mission benefits of fuel specific energy improvements may be realized through either increased range at a given take off gross weight, or reduced weight/additional payload capability for a given mission range.

Table 4
Trade Study Summary.

Case	ΔWeight[†]	ARES	ΔRange (nm)	Fuel Temperature
A	−0.75 %	1.8 %	105	no change
B	−1.3 %	3.2 %	190	no change
C	−1.0 %	2.3 %	139	no change
D	Not feasible		fuel temperature ≈ cabin temperature	
E	Not feasible		fuel temperature exceeds safety limits	
F	−400 to −500 lbs	0.30 %	15	120 ℃

[†] Aircraft maximum gross weight

Theoretical mission benefits of fuel energy density improvements were estimated assuming aircraft outer mold line re-optimization for reduced fuel tank volumes (noting that the aircraft outer mold line is not typically driven by fuel tank volumes in most aircraft), as described in Section 2.7. Energy density benefits are likely to be more beneficial for aircraft that are volume-limited, though nearly all aircraft are weight limited at their maximum range.

Fuel cannot be used as the coolant in the ECS because the fuel temperature exceeds the temperature of cooling set by the cabin. Specifically, fuel cooling was determined to be infeasible for use in the ECS precooling because local fuel temperatures would exceed 260 °C locally (e.g., due to high bleed air temperatures) and because it would result in temperature differentials that are inefficient for cooling., particularly near the end of the mission when fuel levels are at their lowest. Alternatively, architectures (such as a recirculation loop) that could potentially mitigate these issues would detract from the benefit. A potential benefit was identified for using a higher thermal stability fuel to cool higher pressure hydraulic systems. Hydraulic systems that run at higher pressures are net lower weight, but these have higher heat rejection needs given that higher pressures result in more thermal energy within the hydraulic fluid. For example, a 5,000 psi system may have a net weight benefit approximated at 400 to 500 lbs over a 3,000 psi system, realized due to smaller tube volumes and lower volume of hydraulic fluid. However, the higher pressure system could add as much as 60 % more heat to the working fluid. Increasing the fuel exit temperature 65℃ to 120℃ results in more than 80 % reduction in fuel required for cooling. All of the values reported in Table 4 should be considered best-case scenarios.

3.2. Limiting properties and enthalpy impact

Aircraft relative enthalpy savings (ARES), for the representative case, can be improved by up to 0.40 % relative to nominal petroleum-derived JetA by using fuel that has been optimized for efficiency. However, the virtual SAF composition affording that level of improvement does not meet all of the requirements of ASTM D7566. Notably, the aromatics concentration is too low. Upon filtering the solutions shown graphically in Fig. 2 to a minimum aromatics concentration of 8.0 %v, the remaining best-case fuel composition results in ARES = 0.33 %. This composition, as is the case for most of the solutions shown in Fig. 2, is limited by vapor pressure at 160 °C. The energy density of this solution is 34.3 GJ/m^3 which is within the experience range of petroleum-derived JetA (34.0–35.6 GJ/m^3, 95 % confidence interval) [22]. Indeed, all of the calculated properties of this solution fall within the experience range of petroleum jet fuel and therefore it can be considered as a potential drop-in, 100 % SAF candidate (SAF100). Table S1 in the supplemental material contains all of the calculated properties of all of the optimized compositions discussed in this article, including the overall best-case, 100 % drop-in candidate from the LHV/ERES optimization starting with the full 1121 molecule database.

Upon inspection of the species identified as favorable by the initial, full database LHV/ERES optimization, a sub-set database containing only *iso*-alkanes with a single branch was used in place of the full database, and the optimization was repeated. The main results of that optimization are summarized in Fig. 3. The ARES ranges from 0.37 to 0.38 %, and the solutions were limited by mass density. In order to simultaneously provide relief on the mass density and recover some of the fuel/elastomer interactions present with petroleum-derived JetA, these solutions were incrementally seeded with up to 20 %$_{mol}$ ethylbenzene, and the optimization was restarted. The main results of this optimization are shown with circular symbols in Fig. 2. The most favorable (ARES = 0.40 %) Jet-X candidate was found by this optimization, and the most favorable (ARES = 0.32 %) SAF100 candidate identified by this optimization has properties that closely align with those of the LHV/ERES optimization over the full database. Interestingly, the addition of ethylbenzene to the single-branch *iso*-alkane

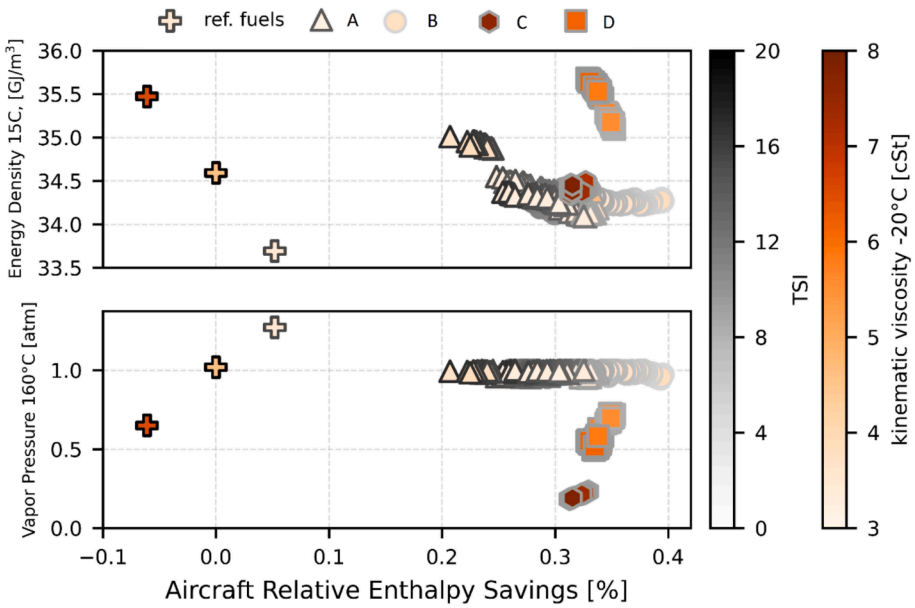

Fig. 2. Jet-X optimization summary a) results from an LHV/ERES optimization using the full database, b) results from an LHV/ERES optimization using database consisting of ethylbenzene and 79 *iso*-alkanes with a single branch, c) results from a Pvap/ARES optimization using the full database, d) results from an ED/ARES optimization using the full database.

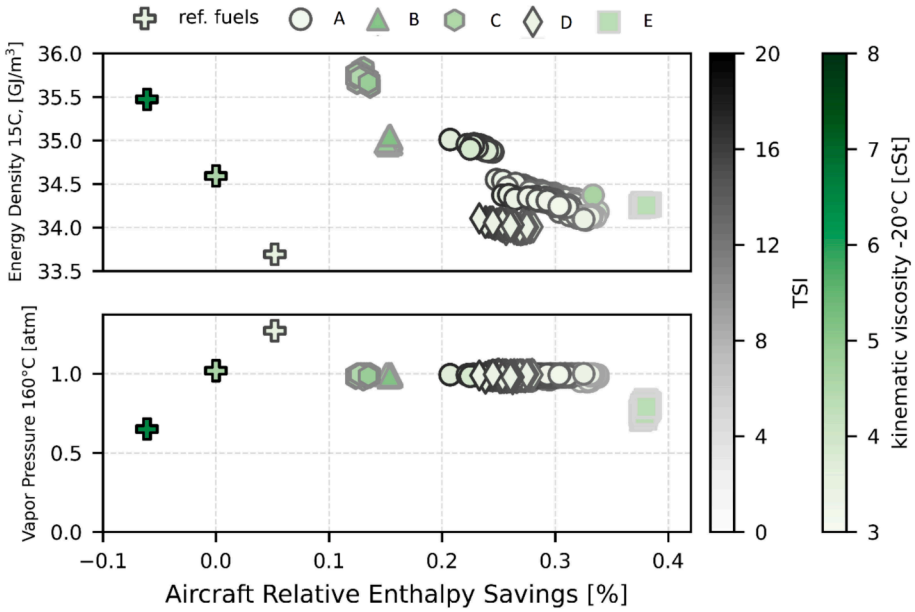

Fig. 3. Results from LHV/ERES optimizations. a) full database, b) database containing only mono-cycloalkanes, c) database containing only mono-, bi- and tri-cycloalkanes, d) database containing no cycloalkanes, e) database containing 79 *iso*-alkanes with a single branch.

database was sufficient to move the limiting property from mass density to vapor pressure, and by providing some relief to the mass density limit, the algorithm shifted the population distribution of *iso*-alkanes toward lower molecular weight species. This shift recovered some LHV lost by seeding ethylbenzene into the pareto front and further reduced the viscosity relative to the reference petroleum fuel. The net result of these changes was a small improvement in both ARES and energy density relative to the database which contained only *iso*-alkanes.

The next dual-objective optimization involved ARES and energy density (ED) because none of the prior optimizations afforded any solutions with higher (more favorable) energy density than that of petroleum-derived JetA. These solutions ranged from ARES = 0.33 to 0.35 % and ED = 35.1 to 35.7 GJ/m^3. Based on input from Boom, an aircraft designed for Jet-X with a lower limit on ED that is shifted 3.2–4.9 % upwards relative to the lower boundary of the 95 % experience range of petroleum jet fuel, would consume 1.3–2.0 % less fuel (enthalpy basis) than an aircraft designed to conventional fuel properties. The predicted fuel properties of these solutions are comparable to those of petroleum-derived JetA except for those properties such as thermal stability, elastomer compatibility, sooting, lubricity, dielectric constant, etc. that depend strongly on aromatics, as only trace levels of aromatics were retained by the optimization algorithm. Among the properties influenced by aromatics, only lubricity is improved by their presence, and we suggest that additives should be used to bring the lubricity of Jet-X into acceptable limits. Note that we are making a presumption here that molecules (such as aromatics) that are absorbed by

O-rings contribute materially to their deteriorated condition after thousands of missions and that it is only such deteriorated O-rings that technically require swell-inducing molecules to maintain an effective seal throughout their duty cycle. The operational requirement is, 'no leaks'. The (as yet unwritten) technical requirement on the fuel should be conceived as a limit on the range of acceptable seal swell values, rather than a minimum swell value (or minimum aromatics content) with an implicit assumption that the maximum swell value corresponds to the worst-case petroleum-derived fuel. We further presume that fuel system quantity indicating systems for aircraft fuel gaging can be readily adapted for any value of fuel dielectric constant and its temperature derivative in the case of aircraft redesign.

The remaining optimization summarized in Fig. 2 involves maximizing ARES while minimizing the vapor pressure at 200 °C. The candidate fuels identified by this optimization are intended for hot fuel applications. The idea is to maximize the liquid fuel's tolerance for heat absorption (without boiling) while adhering to the T_{10} specification of ASTM D1655. Notionally, engine-level altitude relight requirements can be met provided that the fuel meets all of the operability-influencing fuel property specifications/constraints which are vapor pressure, viscosity, and density. The T_{10} ruler constraint that was supplied to the algorithm for this optimization was altered to 0.15 (instead of 0.10) because intermediate solutions (when the ruler limit was set to 0.10) were found to have unacceptable T_{10} values. The actual T_{10} is computationally more cumbersome to estimate because it requires a simulated distillation, while the T_{10} ruler requires only a sorting operation on boiling point. This is why the T_{10} ruler, rather than the actual T_{10}, is part of the constraint filter, noted in Fig. 1. The viscosity at −20 °C and the T_{10} ruler are both limiting properties as far as the algorithm is informed of the fuel quality requirements.

In spite of meeting specification requirements, this fuel is a risk to cold start and altitude relight requirements for two reasons: high viscosity and low vapor pressure. The converged ARES/P_{vap} solutions afford no better ARES (0.31–0.33 %) than the ARES/ED solutions and their energy density is lower. Nevertheless, we entertain the possibility (no matter how unlikely) that the extra design envelope afforded by such a fuel with regard to the aircraft or engine thermal management system could trump the somewhat larger fuel tanks and tubing requirements (relative to the ARES/ED solutions) and whatever provisions are necessary to ensure altitude relight capability. To the extent that the following models and approximations are accurate, the vapor pressure (P_{vap}) of the fuel at any temperature (T) is given by equation (8), where T_b is the normal boiling point. These models and approximations include Trouton's Rule, Raoult's Law, Daltons Law, and the Clausius-Clapeyron Equation.

$$P_{vap} = exp(10.404 * \left(1 - \frac{T_b}{T}\right)) \tag{8}$$

Inherently, any fuel with an elevated boiling point will have exponentially lower vapor pressure (and evaporation rates) as combustor inlet temperatures decrease. Relative to 156 °C (which is chosen here as a reference because it corresponds to the mean bubble point of 4901 JP8 samples reported in the 2011 PQIS database [22]) the vapor pressure at −20 °C of a fuel with a normal boiling point of 200 or 250 °C is 1.76 or 13.7 times lower, respectively. Such a large impact on vapor pressure is expected to result in a large deleterious impact on the fuel evaporation rate at combustor inlet conditions corresponding to cold-day ignition. As a result, fuel like those resulting from the ARES/P_{vap} optimization would place a premium on thermal management design concepts that avoid the need to select a fuel with decreased fuel vapor pressure at high temperature. This can be done by avoiding the transfer of too much heat into the fuel at low-flow operating conditions (low fuel pressure) while enabling the transfer of as much heat as possible into the fuel at high-flow operating conditions (high fuel pressure).

3.3. Composition characteristics of Jet-X and optimized SAF100 candidates

The prominent composition characteristics of the average of each pareto front shown in Fig. 2 are discussed below while the detailed composition of any point shown in this manuscript is available upon request.

The full database LHV/ERES optimization favored *iso*-alkanes (77.8 $\%_{mol}$) over all other all other hydrocarbon types. In particular, 3-ethyldecane accounted for 17.0 $\%_{mol}$ of the average composition and was the only compound present at greater than 10 $\%_{mol}$. As evident from Fig. 4, the optimization favored *iso*-alkanes with one or two branches, together accounting for 65.3 $\%_{mol}$ of the pareto front solutions. The average molecular weight of the alkanes in the pareto front was found to be 151.0 g/mol, with notably higher weighting of species with 10 or 12 carbon atoms. The relative paucity of *iso*-alkanes with 11 carbon atoms within the pareto is not yet fully explained and should not be taken too literally. Part of the reason could be that the full database contained 71, 43, and 48 different *iso*-alkanes with 10, 11, and 12 carbon atoms, respectively. Also, 3-ethyldecane has a normal boiling point of 204.6 °C, just under the T_{10} constraint of 205 °C, which could be artificially favored as a result of the approximations used to account for this constraint. Cycloalkanes, including mono- bi- and tri-cycloalkanes comprised just 9.7 $\%_{mol}$ of the pareto front solutions. Among the cycloalkanes, nearly all contained a 5-membered ring and nearly half were comprised of species without any alkyl group branching. The average molecular weight of the identified cycloalkanes was quite low, with carbon number (C#) ranging from 7 to 10. The most prominent cycloalkane was bicyclo[2.2.1]heptane, which accounted for 2.5 $\%_{mol}$ of the pareto front average. Aromatics, including alkylbenzenes, naphthalenes, indanes and tetralins constituted 12.5 $\%_{mol}$ of the pareto front solutions. Nearly all of these were alkylbenzenes. While no single aromatic molecule exceeded 3 $\%_{mol}$, those with a total of 12 carbon atoms accounted for nearly half of all aromatic content.

The LHV/ERES optimization initiated from a database containing ethylbenzene and 79 *iso*-alkanes with one branch resulted in an average (of 250 points) pareto front that contained 11.3 $\%_{mol}$ ethylbenzene and 88.7 $\%_{mol}$ *iso*-alkanes. The carbon number distribution, shown in Fig. 5, of the *iso*-alkanes in these solutions was found to have much in common with the result from the LHV/ERES optimization over the full database. Like the former optimization, two molecules, 3-ethyldecane (19.1 $\%_{mol}$) and 3-ethyloctane (15.3 $\%_{mol}$) had significantly elevated concentrations relative to other species. However, one molecule, 6-pentyldodecane (9.3 $\%_{mo}$) was favored by this optimization but not favored in the similar optimization over the full database. This observation illustrates that solutions are not unique, and that potential short-comings of one solution can be overcome with little or no loss of performance benefit. For example, if one solution has a freeze point that is too high because of too much concentration of one or another high-freeze-point component, such as 3-ethyldecane or 6-pentyldodecane, its concentration can be restricted to an acceptable level in a subsequent optimization which will find an alternative composition that is nearly as good. This example demarcates a genuine risk with each of these Jet-X candidates. The reported freeze point of 3-ethyldecane is 72 °C [23] and the freeze point of 6-pentyldodecane is suspected to be significantly higher than −40 °C, which is the maximum allowable freeze point of JetA fuel per ASTM D1655. At present, no supplier of these materials (at any grade) has been found, rendering it problematic to quantify this risk. Moreover, a pathway to the cost-effective producibility of these materials is beyond the scope of this article.

The ARES/ED optimization that began with the full database containing 1121 molecules, also favored *iso*-alkanes (91.4 $\%_{mol}$) over all other all other hydrocarbon types. The two most favored molecules by this optimization were 3-ethyldecane (14.9 $\%_{mol}$) and 5,10-dimethyltetradecane (7.1 $\%_{mol}$), and a total of 28 molecules were present at concentration higher than 1 %. The averaged compositions across each of

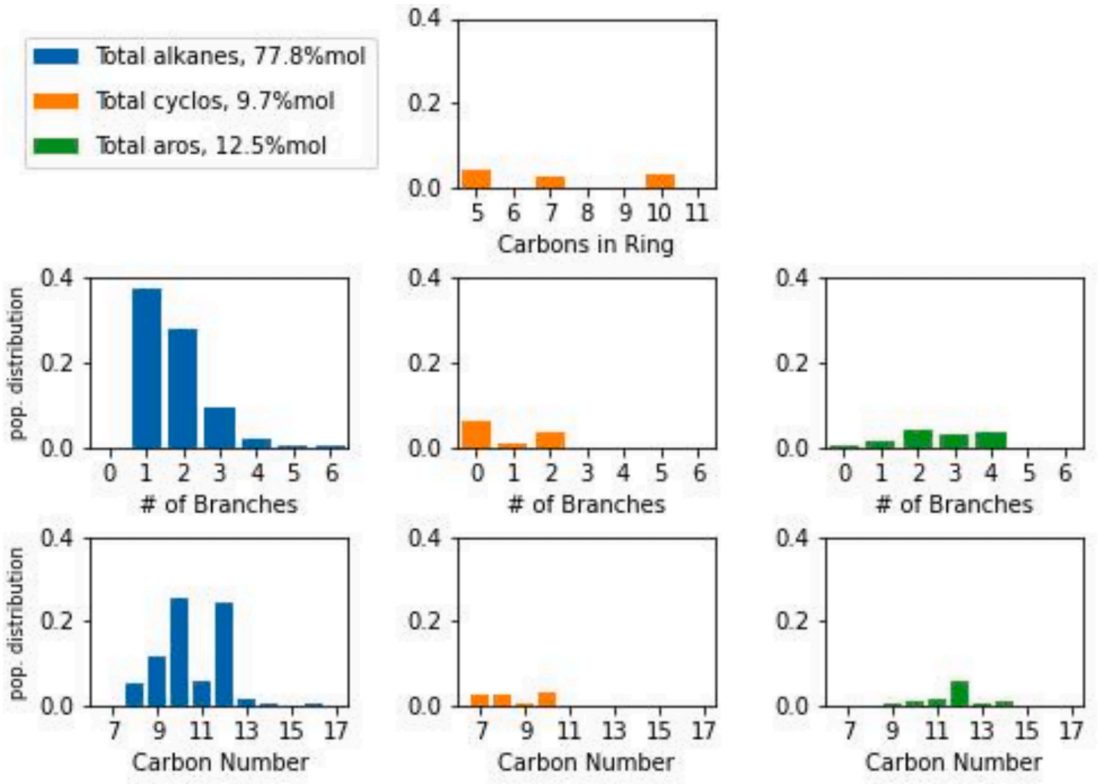

Fig. 4. Composition characterization: result of an LHV/ERES optimization using the full database. Carbons-in-rings is defined as the total number of carbon atoms that are linked into a ring, including mono-, bi-, and tri-cycloalkanes. The total mole percentage of species with a degree of unsaturation (DoU) equal to 2, 3, 5, or 7 is 3.6 % $_{mol}$, where DoU is defined as: (1 + C# − H#/2).

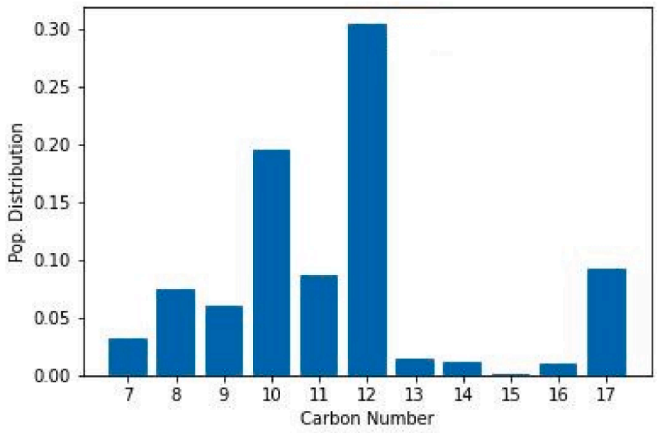

Fig. 5. Composition characterization: result of an LHV/ERES optimization using a database containing ethylbenzene and 79 *iso*-alkanes with a single branch. The four most abundant species, on average, in this set of 250 compositions are: 3-ethyldecane (19.1 %$_{mol}$), 3-ethyloctane (15.3 %$_{mol}$), ethylbenzene (11.3 %$_{mol}$), and 6-pentyldodecane (9.3 %$_{mol}$).

the pareto fronts presented in Fig. 2 are provided in Table S2 within the supplemental material. A notable advantage of a fuel with many constituents is that its freeze point should be quite low. However, the producibility of such a fuel, precisely as defined by the optimized compositions, is challenging. The path forward here is to produce mixtures that reproduce the higher-level composition characteristics shown in Fig. 6 as closely as is pragmatic while also targeting specific representation of the most prevalent species in these definitions.

While 3-ethyldecane was highlighted by all of the optimizations, clear compositional differences exist between those solutions optimized for LHV and ERES and those optimized for ED and ARES. The ED/ARES optimized candidates contain essentially no aromatic materials, instead containing *iso*-alkanes with higher molecular weight (174.6 g/ml compared to 152.3 g/ml) and more branching than their LHV/ERES optimized counterparts. The characteristics of the selected cycloalkanes also differed significantly. The ED/ARES optimization identified significant content of compounds with 8-, 9- and 10-membered rings in addition to one bridged ring compound, bicyclo[3.3.3]undecane. Conversely, the LHV/ERES optimization identified primarily cyclopentanes and di-cyclopentanes. The often-discussed molecule, decalin [24–26] was present in the full database, but was not selected by any of the optimizations.

The ARES/P_{vap} @200 °C optimization that began with the full database containing 1121 molecules favored *iso*-alkanes (99.9 %$_{mol}$) to the exclusion of all other hydrocarbon types. The most favored molecule was again 3-ethyldecane, which comprised 9.4 %$_{mol}$ of the pareto front solutions. The second and third most favored molecules in this pareto front were 6-pentylundecane (2.8 %) and 5-propylundecane (2.5 %), respectively. Overall, 32 molecules were identified in concentration over 1 %, and the average molecular weight of these Jet-X candidates was determined to be 193.7 g/ml. Iso-alkanes with 1 or 2 branches comprised 76 %mol of the pareto front solutions, which can be seen graphically in Fig. 7. In addition to the property risks noted above, namely viscosity and vapor pressure at arctic-day conditions, the cost-effective producibility of this mixture is a very high risk. While the mixture contains many species from a production point of view, the total number of isomers represented in these solutions is a small fraction of all possible isomers of *iso*-alkanes. Moreover, it is unlikely that the optimal proportions of these molecules match those of any known production pathway as separation of the favored isomers relative to the unfavored isomers would be challenging. Nonetheless, this optimization affords a benchmark of best-case performance benefit which is useful for charting a course to net-zero CO_2 emissions by 2050 even if a different path is

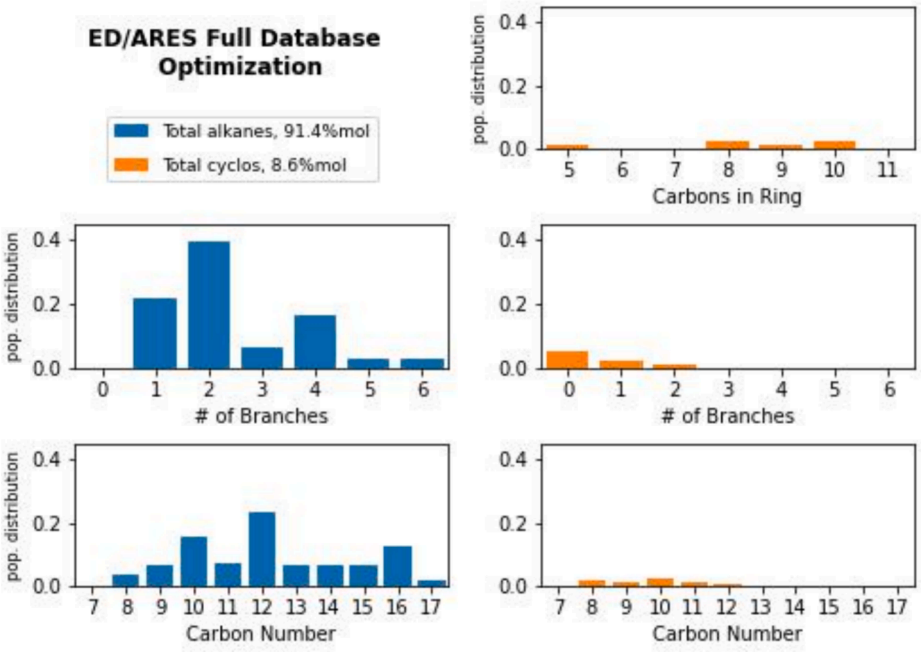

Fig. 6. Composition characterization: result of an ED/ARES optimization using the full database. Carbons-in-rings is defined as the total number of carbon atoms that are linked into a ring, including mono- and bi- (or di-) cycloalkanes.

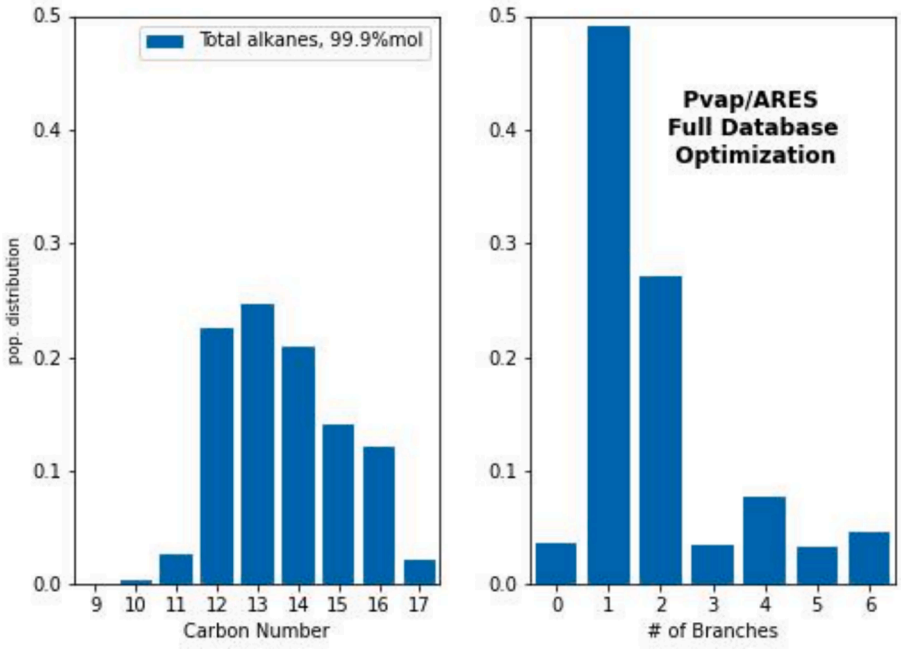

Fig. 7. Composition characterization: result of P_{vap} / ARES optimization using the full database.

pursued.

4. Conclusion

Sustainable aviation fuel is required by quality-controlling specifications to meet a higher thermal stability standard than petroleum distillate fuels and this characteristic can be leveraged to improve energy efficiency in new or *retro*-fitted engine or aircraft designs where a commitment has been made to burning fuel that meets a specification beyond that of conventional JetA (e.g. ASTM D1655). Additionally, Jet-X developers have the opportunity to further increase the value of their product by infusing higher-than-conventional-Jet-A specific energy into the fuel they produce, with marginal added value for increased energy density. This work shows that fuel energy density can be increased 3.2–4.9 % relative to -2σ JetA (2011, PQIS data) while simultaneously increasing its specific energy by 1.0 %. While the direct (a.k.a. drop-in) impact of higher specific energy on aircraft efficiency is 0.43 % per MJ/kg increase in LHV for a *trans*-ocean flight in a legacy supersonic aircraft, Boom has estimated 1.8 % enthalpy savings is possible with redesign to leverage an increase in fuel specific energy of 2 %. While increases in fuel energy density could have aircraft enthalpy savings, aircraft development potential with reduced tank volumes is typically

constrained by other factors such as wing packaging, passenger volume requirements and overall center of gravity and flight control law restrictions. Further, increased energy density fuels are likely to have limited value for weight-limited aircraft (which applies to most current aircraft including supersonic aircraft) where fuel tanks are designed to have excess volumetric capacity at maximum range. Absent any design change whatsoever to the engine, aircraft, or airport fuel-hydrant hardware, SAF100 can be optimized to afford approximately 0.3 % better fuel economy depending on the specific aircraft and its assigned mission.

Iso-alkanes have been identified as the most preferred hydrocarbon type from an enthalpy consumption perspective. Iso-alkanes with one or two branches were favored when energy density was ignored and the minimum mass density requirement was met by blending with aromatics and cycloalkanes. In this case, fuel vapor pressure at 160 °C motivated the carbon number population distribution of the *iso*-alkanes and blend components alike. The *iso*-alkane fraction of these solutions had an average molecular weight of 152.3 g/mol. The cycloalkane fraction of these solutions consisted primarily of compounds with one or two five-membered rings, and the aromatic fraction consisted primarily of molecules containing a total of 12 carbon atoms. However, a similar enthalpy efficiency impact was attained for optimized SAF with no cycloalkanes and just one aromatic compound, ethylbenzene. In this case the average molecular weight of the *iso*-alkane fraction was 151.0 g/mol and that was motivated by a combination of mass density and vapor pressure.

For the dual-objective optimization of energy density and aircraft relative enthalpy savings, the population distribution of *iso*-alkanes, relative to the prior optimization case, shifted to higher molecular weight (174.6 g/mol) and increased branching. The characteristics of the cycloalkanes in these candidate fuels also shifted relative to the prior optimization. In this case, several mono-cycloalkanes containing ring structures with 8, 9, or 10 carbon atoms showed up as promising components in Jet-X. The drawback of increased energy density was found to be increased viscosity, but 25 % margin (6 cSt compared to 8 cSt) to the maximum allowed viscosity for JetA at −20 °C remained. Moreover, the vapor pressure (*ca.* 0.22 torr) at −20 °C remained reasonable.

Designing a fuel to maximize the allowable fuel temperature by minimizing vapor pressure at 200 °C proved problematic since the vapor pressure at −20 °C (<0.09 torr) drops below the industry experience range, presenting a significant risk to arctic-day ignition requirements, and the viscosity was driven all the way up to its maximum limit, which further increases the risk to both arctic-day ignition as well as altitude relight conditions. The lesson here is not that hot fuel cannot be done, but rather that design changes intended to exploit the higher thermal stability of SAF should not add much additional heat into the fuel at conditions corresponding to low fuel pressure, instead allowing much more heat into the fuel when the fuel pressure is well above the critical pressure of the fuel such that the change in fuel (mass) density with temperature remains sufficiently low to avoid fuel flow control system instabilities, cavitation and fuel-coupled combustion dynamics.

CRediT authorship contribution statement

Randall C. Boehm: Writing – review & editing, Writing – original draft, Software, Project administration, Methodology, Investigation, Formal analysis, Data curation, Conceptualization. **Conor Faulhaber:** Writing – review & editing, Visualization, Data curation. **Lily Behnke:** Writing – original draft, Software, Methodology. **Joshua Heyne:** Project administration, Funding acquisition, Writing – review & editing.

Declaration of competing interest

The authors declare that they have no known competing financial interests or personal relationships that could have appeared to influence the work reported in this paper.

Data availability

Data is provided in the supporting material.

Acknowledgments

This research was funded by the United States Federal Aviation Administration (FAA) Office of Environment and Energy through ASCENT, the FAA Center of Excellence for Alternative Jet Fuels and the Environment, project 66 through FAA Award Number 13-C-AJFE-WaSU-036 under the supervision of Prem Lobo and Ana Gabrielian. Any opinions, findings, conclusions or recommendations expressed in this material are those of the authors and do not necessarily reflect the views of the FAA. Contributions from Boom Technology, Inc. have been noted in the manuscript and are formally acknowledged here as well. Furthermore, we would like to acknowledge Harrison Yang for his guidance in python coding of fuel blending rules and the EPM and FSTM.

Appendix A. Supplementary data

Supplementary data to this article can be found online at https://doi.org/10.1016/j.fuel.2024.132049.

References

[1] Air Transportation Action Group: ATAG. Waypoint 2050. vol. Second Edi. Geneva, Switzerland: 2021.
[2] Lee DS, Fahey DW, Skowron A, Allen MR, Burkhardt U, Chen Q, et al. The contribution of global aviation to anthropogenic climate forcing for 2000 to 2018. Atmos Environ 2021;244:117834. https://doi.org/10.1016/J.ATMOSENV.2020.117834.
[3] Goldner W, Bredlau J, Brown N, Haq Z, Brown C, Inter-agency-team. SAF Grand Challenge Roadmap: Flight Plan for Sustainable Aviation Fuel. n.d.
[4] Kosir S, Stachler R, Heyne J, Hauck F. High-performance jet fuel optimization and uncertainty analysis. Fuel 2020;281:118718. https://doi.org/10.1016/j.fuel.2020.118718.
[5] Kosir S, Heyne J, Kirby M. High-performance jet fuel optimization and aircraft performance analysis considering o-ring volume swell. Columbia, South Carolina: Spring Tech. Meet. East. States Sect. Combust. Inst; 2020.
[6] Kroyan Y, Wojcieszyk M, Kaario O, Larmi M. Modeling the impact of sustainable aviation fuel properties on end-use performance and emissions in aircraft jet engines. Energy 2022;255:124470. https://doi.org/10.1016/J.ENERGY.2022.124470.
[7] Boehm RC, Scholla LC, Heyne JS. Sustainable alternative fuel effects on energy consumption of jet engines. Fuel 2021;304:121378. https://doi.org/10.1016/J.FUEL.2021.121378.
[8] Edwards T. Reference jet fuels for combustion testing. In: AIAA SciTech Forum - 55th AIAA Aerosp. Sci. Meet. Grapevine, TX: American Institute of Aeronautics and Astronautics Inc; 2017. p. 1–58. https://doi.org/10.2514/6.2017-0146.
[9] Colket M, Heyne J, Rumizen M, Gupta M, Edwards T, Roquemore WM, et al. Overview of the national jet fuels combustion program. Https://DoiOrg/102514/1J055361 2017;55:1087–104. https://doi.org/10.2514/1.J055361.
[10] Guildenbecher DR, López-Rivera C, Sojka PE. Secondary atomization. Exp Fluids 2009;46:371–402. https://doi.org/10.1007/s00348-008-0593-2.
[11] Mellor AM. Design of modern turbine combustors. San Diego, CA: Academic Press; 1990.
[12] Lemmon EW, Bell IH, Huber ML, McLinden MO. NIST standard reference database 23. Reference Fluid Thermodynamic and Transport Properties-REFPROP 2018.
[13] Heyne J, Rauch B, Le Clercq P, Colket M. Sustainable aviation fuel prescreening tools and procedures. Fuel 2021;290:120004. https://doi.org/10.1016/j.fuel.2020.120004.
[14] Bell D, Heyne JS, August E, Won SH, Dryer FL, Haas FM, et al. On the development of general surrogate composition calculations for chemical and physical properties. AIAA SciTech Forum - 55th AIAA Aerosp Sci Meet 2017. https://doi.org/10.2514/6.2017-0609.
[15] Flora G, Kosir S, Behnke L, Stachler R, Heyne J, Zabarnick S, et al. Properties calculator and optimization for drop-in alternative jet fuel blends. AIAA Scitech 2019 Forum. American institute of aeronautics and astronautics Inc, AIAA; 2019. 10.2514/6.2019-2368.
[16] Gill RJ, Olson DB. Estimation of soot thresholds for fuel mixtures. Combust Sci Technol 1984;40:307–15. https://doi.org/10.1080/00102208408923814.
[17] Moses C. Research for the aerospace systems directorate (R4RQ) delivery order 0006: Airbreathing propulsion fuels and energy exploratory research and development (APFEERD) Subtask: Review of bulk physical properties of synthesized hydrocarbon: Kerosenes and blends. Oh: Wright-Patterson Air Force Base; 2017.

[18] Hugill JA, Van Welsenes AJ. Surface tension: A simple correlation for natural gas + conensate systems. Fluid Phase Equilib 1986;29:383–90. https://doi.org/10.1016/0378-3812(86)85038-5.
[19] Wilding WV, Rowley RL, Oscarson JL. DIPPR® Project 801 evaluated process design data. Fluid Phase Equilib 1998;150–151:413–20. https://doi.org/10.1016/S0378-3812(98)00341-0.
[20] Boehm RC, Coburn AA, Yang Z, Wanstall CT, Heyne JS. Blend prediction model for the freeze point of jet fuel range hydrocarbons. Energy Fuel 2022;36:12046–53. https://doi.org/10.1021/acs.energyfuels.2c02063.
[21] Faulhaber C, Borland C, Boehm R, Heyne J. Measurements of nitrile rubber absorption of hydrocarbons: Trends for sustainable aviation fuel compatibility. Energy Fuel 2023;37:9207–19. https://doi.org/10.1021/acs.energyfuels.3c00781.
[22] Martin D, Wilkins P. Petroleum quality information system (PQIS) 2011 annual report. Fort Belvoir, VA: Defense Technical Information Center; 2011.
[23] Petrov AD, Pavlov AM, Makarov YA. Synthesis of 3-ethyldecane and of 2, 5-dimethylhendecane. Zh Obs Khim 1941;2:1104–6.
[24] Liu Y, Wilson CW. Investigation into the impact of n-decane, decalin, and isoparaffinic solvent on elastomeric sealing materials. Adv Mech Eng 2012;2012. https://doi.org/10.1155/2012/127430.
[25] Muldoon JA, Harvey BG. Bio-based cycloalkanes: The missing link to high-performance sustainable jet fuels. ChemSusChem 2020;13:5777–807. https://doi.org/10.1002/CSSC.202001641.
[26] Undavalli V, Gbadamosi Olatunde OB, Boylu R, Wei C, Haeker J, Hamilton J, et al. Recent advancements in sustainable aviation fuels. Prog Aerosp Sci 2023;136:100876. https://doi.org/10.1016/j.paerosci.2022.100876.

Technical Report Documentation Page

1. Report No.	2. Government Accession No.	3. Recipient's Catalog No.
j.fuel.2024.132049		

4. Title and Subtitle	5. Report Date
The effect of theoretical SAF composition on calculated engine and aircraft efficiency	June 2024
	6. Performing Organization Code

7. Author(s)	8. Performing Organization Report No.
Randall C. Boehm, Conor Faulhaber, Lily Behnke, Joshua Heyne	

9. Performing Organization Name and Address	10. Work Unit No. (TRAIS)
Center of Excellence for: Alternative Jet Fuels and Environment Washington State University, Pullman, WA 99164	11. Contract or Grant No. 13-C-AJFE-WaSU-036

12. Sponsoring Agency Name and Address	13. Type of Report and Period Covered
Federal Aviation Administration Office of Environment and Energy	Journal Article
	14. Sponsoring Agency Code

15. Supplementary Notes

16. Abstract

Whether the feedstock for sustainable aviation fuel (SAF) originates from agriculture or from waste streams, life cycle CO2 emissions per unit enthalpy are lower for SAF than they are for petroleum distillates primarily because of differences on the front end such as fostered growth of crops or decreased demand for resources or acreage to manage wastes. This work, however, is concerned with what happens on the consumption side. Sustainable aviation fuel is required by ASTM D4054 / D7566 to meet a higher thermal stability standard than petroleum distillate fuels and this characteristic can be leveraged to improve energy efficiency in new engine or aircraft designs where a commitment has been made to burning fuel that meets a specification beyond that of conventional JetA. Beyond thermal stability, non-drop-in SAF (Jet-X) developers have the opportunity to further increase the value of their product by infusing higher-than-conventional-JetA energy density (enthalpy per unit volume, ED) into their SAF. Finally, fuel specific energy (enthalpy per unit mass, LHV) has a direct impact on aircraft efficiency which we have determined to be 0.43% per MJ/kg increase in LHV depending on the mission and aircraft model, and this is applicable to both drop-in and non-drop-in applications. While higher energy density fuels may be leveraged in a new aircraft design to decrease drag and weight, aircraft development potential with reduced tank volumes is typically constrained by other factors such as wing packaging, passenger volume requirements and overall center of gravity and flight control law restrictions.

17. Key Words	18. Distribution Statement
Sustainable Aviation Fuel, Energy Efficiency, Composition Optimization, ASCENT	

19. Security Classif. (of this report)	20. Security Classif. (of this page)	21. No. of Pages	22. Price
Unclassified	Unclassified		